



ELSEVIER

Available online at www.sciencedirect.com

SCIENCE @ DIRECT®

Journal of Sound and Vibration 280 (2005) 289–310

JOURNAL OF
SOUND AND
VIBRATION

www.elsevier.com/locate/jsvi

An analysis of a vibratory angular-rate gyroscope using polarized piezoceramic bimorph plates. Part 2: solution procedure for the gyroscope with superposed angular velocity

Jongwon Seok*, H.F. Tiersten, H.A. Scarton

Department of Mechanical, Aerospace and Nuclear Engineering, Rensselaer Polytechnic Institute, 110 8th Street, Troy, NY 12180-3590, USA

Received 16 October 2002; accepted 4 December 2003

Abstract

The variational equations derived in Part 1 of this work are extended to include the superposed angular velocity by means of the Coriolis effect. The resulting equations enable a semi-analytic treatment for the calculation of the dynamic characteristics of a vibratory angular-rate gyroscope composed of small piezoceramic bimorphs arranged in the shape of one half of a single tuning fork; use of mirror symmetries of that basic shape allows the construction of an H-shaped tuning fork gyroscope. The calculations are performed at the resonant frequency of the fundamental flexural mode. The dimensions of a typical half of a tuning fork shape structure considered in this work are approximately $2.6 \text{ mm} \times 0.88 \text{ mm} \times 0.16 \text{ mm}$, which has fundamental natural frequencies ranging between 5 and 8 kHz, and can measure rotation-rates at least as high as 40 RPM. In order to have greater sensitivity it is necessary to have simultaneously large amplitudes of vibration in both the actuating and sensing modes. On account of this the two forced vibration problems are solved only at the matched first natural frequency of the fundamental flexural mode, which is obtained from the eigenanalysis that enables the selection of geometry for the frequencies to be matched.

© 2004 Elsevier Ltd. All rights reserved.

1. Introduction

Clearly the introduction to Part 1 [1] pertains to this work also and will not be reproduced here. At this point, it is worth noting that the complete analytical formalism required in the treatment is presented in Part 1 in the absence of the angular velocity, which the gyroscope is intended to

*Corresponding author. Currently: Assistant Professor, School of Mechanical Engineering, College of Engineering, Chung-Ang University, 221, Heukseok-Dong, Dongjak-Gu, Seoul 156-756, Korea. Tel.: +82-31-215-3319; fax: +82-31-215-3319.

E-mail address: seokj@alum.rpi.edu (J. Seok).

measure. However, no solution functions are presented in Part 1, nor were any results of calculations presented.

In this work the analytical formalism is extended to include the angular velocity in the sensing vibration mode. In addition, all solution functions required in each region of the gyroscope are obtained here and some numerical results are presented and discussed. In particular, the semi-analytic treatment developed in these works is employed in the calculation of the optimal design conditions for equal resonances of the actuating and sensing modes along with the sensitivity as a function of the superposed angular velocity for a range of quality factors.

2. Solution procedure for a forced vibration problem of a half tuning fork shape gyroscope

2.1. Development of variational equations of the system under rotation

The tuning fork described in Fig. 1 of Ref. [1] now rotates with a constant rotation-rate Ω about the $x_1^{(A)}$ axis. The position vector of the point of the body P at the generic time t is given by

$$\mathbf{y} = \mathbf{x} + \mathbf{u}. \quad (1)$$

Here, \mathbf{x} is the position vector from the origin of the body axes to a point of the body in the undeformed state, \mathbf{u} is the deformation vector, \mathbf{y} is a position vector from the origin of the body axes to the point of the deformed body.

Since Hamilton's principle is valid only for holonomic systems, non-holonomic kinematical conditions cannot be included in the energy function [2], because non-holonomic constraints are differential relations not derivable from a functional. However, the motion of such a system can be taken into account by extending Hamilton's principle to include the virtual work due to the nonholonomic conditions in a d'Alembertian manner.

The d'Alembert inertia force $d\mathbf{F}_I$ induced by the rotation of the mass with the angular velocity Ω included in volume dV has the form

$$d\mathbf{F}_I = -2\rho(\Omega \times \dot{\mathbf{u}}) dV - \rho\Omega \times (\Omega \times \mathbf{y}) dV. \quad (2)$$

It should be noted that the motion of the reference frame gives rise to two apparent forces having different characters. The first force in the right-hand side of Eq. (2) is the Coriolis force, which depends on the velocity of the moving point and the second force is the centrifugal force, which depends on the position of the point and is ignored in this work since $|\Omega| \ll \omega$. On account of the foregoing assumptions, the virtual work done by the Coriolis force induced by the rotation of the reference system should be directly added to the virtual work in Eq. (1) of Ref. [1]:

$$\delta W' = \delta W + \delta W^I, \quad (3)$$

where

$$\delta W = \int_S (\bar{\mathbf{t}} \cdot \delta \mathbf{u} + \bar{\sigma} \delta \varphi) dS, \quad \delta W^I = -2 \int_V (\rho \Omega \times \dot{\mathbf{u}}) \cdot \delta \mathbf{u} dV. \quad (4)$$

The substitution of Eq. (3) into Hamilton’s principle to include the Coriolis effect, results in the form

$$\delta \int_{t_0}^t L dt + \int_{t_0}^t \delta W' dt = 0. \tag{5}$$

From Eq. (5), with Eq. (4), and the variational equations (10), (11) and (16), (17) of Ref. [1], we obtain the variational equations with superposed angular velocity for the actuating motion in the form

$$T_1^{RA} + T_2^{RA} + T_3^{RA} = 0, \tag{6}$$

where

$$\begin{aligned} T_1^{RA} \doteq & \int_{t_0}^t dt \left[\int_S dS \left[\left\{ \tau_{rz,r}^{(0)} + \frac{\tau_{\theta z,\theta}^{(0)} + \tau_{rz}^{(0)}}{r} - 2\rho h \left\{ \overset{(1)}{v} - 2\Omega \left(\cos \theta \overset{(1)}{\dot{u}}_{\theta}^{(0)} + \sin \theta \overset{(1)}{\dot{u}}_r^{(0)} \right) \right\} \right\} \delta \overset{(1)}{v} \right. \right. \\ & + \left. \left. \left\{ \tau_{rr,r}^{(1)} + \frac{\tau_{r\theta,\theta}^{(1)}}{r} + \frac{\tau_{rr}^{(1)} - \tau_{\theta\theta}^{(1)}}{r} - \tau_{rz}^{(0)} \right\} \delta u_r^{(1)} + \left\{ \tau_{r\theta,r}^{(1)} + \frac{1}{r} \left(\tau_{\theta\theta,\theta}^{(1)} + 2\tau_{r\theta}^{(1)} \right) - \tau_{\theta z}^{(0)} \right\} \delta u_{\theta}^{(1)} \right] \right. \\ & + \int_S dS \left(\tau_{ab,a}^{(2)} - 2\rho h \left(\overset{(2)}{\ddot{u}}_b^{(0)} - 2\delta_{2b}\Omega \overset{(2)}{\dot{w}} \right) \right) \delta u_b^{(2)} + \int_S dS \left\{ \left(\tau_{a3,a}^{(2)} - 2\rho h \overset{(2)}{\dot{w}} \right) \delta \overset{(2)}{w} \right. \\ & + \left. \left(\tau_{ab,a}^{(2)} - \tau_{3b}^{(2)} \right) \delta u_b^{(2)} \right\} + \int_S dS \left\{ \left(\tau_{a3,a}^{(3)} - 2\rho h \left(\overset{(3)}{\dot{w}} + 2\Omega \overset{(3)}{\dot{u}}_2^{(0)} \right) \right) \delta \overset{(3)}{w} \right. \\ & \left. \left. + \left(\tau_{ab,a}^{(3)} - \tau_{3b}^{(3)} \right) \delta u_b^{(3)} \right\} \right], \tag{7a} \end{aligned}$$

$$\begin{aligned} T_2^{RA} \doteq & \int_{t_0}^t dt \left[\int_{-\Theta}^{\Theta} dx_2 \left[r \left\{ \left(\tau_{rz}^{(0)} + \frac{\tau_{r\theta,\theta}^{(1)}}{r} \right) \delta \overset{(1)}{v} - \tau_{rr}^{(1)} \delta \overset{(1)}{\vartheta} \right\} \right] \right]_{x_1=R_i}^{x_1=R_o} \\ & - \int_{-l}^l dx_1 \left[\tau_{21}^{(2)} \delta u_1^{(2)} + \tau_{22}^{(2)} \delta u_2^{(2)} \right]_{x_2=-b}^{x_2=b} \end{aligned}$$

$$\begin{aligned}
 & - \int_{-l}^l dx_1^{(2)} \left[\left(\tau_{23}^{(2)} + \tau_{21,1}^{(2)} \right) \delta w^{(2)} - \tau_{22}^{(1)} \delta \theta_t^{(2)} \right]_{x_2=-b}^{x_2=b} \\
 & - \int_{-l}^l dx_1^{(3)} \left[\left(\tau_{23}^{(3)} + \tau_{21,1}^{(3)} \right) \delta w^{(3)} - \tau_{22}^{(1)} \delta \theta_t^{(3)} \right]_{x_2=-b}^{x_2=b} \Bigg], \tag{7b}
 \end{aligned}$$

$$\begin{aligned}
 T_3^{RA} \doteq & \int_{t_0}^t dt \left[- \int_{R_i}^{R_o} dx_1^{(1)} \left[v \delta \tau_{\theta z}^{(1)} - \vartheta \delta \tau_{r\theta}^{(1)} \right]_{x_2=-\theta}^{(1)} - \left[\tau_{r\theta}^{(1)} \delta v \right]_{x_1=R_i, x_2=-\theta}^{(1)} + \left[\tau_{r\theta}^{(1)} \delta v \right]_{x_1=R_o, x_2=\theta}^{(1)} \right. \\
 & + \left[\tau_{r\theta}^{(1)} \delta \hat{v} + \tau_{r\theta}^{(1)}(r - r_0) \delta \hat{\vartheta} \right]_{x_1=R_i, x_2=\theta}^{(1)} - \left[\int_{R_i}^{R_o} \left(\tau_{\theta z}^{(1)} + \tau_{\theta r, r}^{(1)} \right) dx_1 \cdot \delta \hat{v} - \int_{R_i}^{R_o} \tau_{\theta\theta}^{(1)} dx_1 \cdot \delta \hat{v} \right. \\
 & + \left. \int_{R_i}^{R_o} \left(\tau_{\theta z}^{(1)} + \tau_{\theta r, r}^{(1)} \right) (r - r_0) dx_1 \cdot \delta \hat{\vartheta} \right]_{x_2=\theta}^{(1)} + \left[\int_{-b}^b \tau_{11}^{(2)} x_2 dx_2 \cdot \delta \hat{\psi} - \int_{-b}^b \tau_{12}^{(2)} dx_2 \cdot \delta \hat{u}_2 \right]_{x_1=-l}^{(2)} \\
 & - \left[\int_{-b}^b \left(\tau_{13}^{(2)} + \tau_{12,2}^{(2)} \right) x_2 dx_2 \cdot \delta \hat{\theta}_t \right]_{x_1=-l}^{(2)} - \int_{-b}^b dx_2^{(3)} \left[\left(\tau_{13}^{(3)} + \tau_{12,2}^{(3)} \right) \delta w^{(3)} - \tau_{11}^{(3)} \delta \phi^{(3)} \right]_{x_1=l}^{(3)} \\
 & - \left[\tau_{12}^{(2)} \delta w^{(2)} + \tau_{12}^{(2)} x_2 \cdot \delta \hat{\theta}_t \right]_{x_1=-l, x_2=-b}^{(2)} + \left[\tau_{12}^{(2)} \delta w^{(2)} + \tau_{12}^{(2)} x_2 \cdot \delta \hat{\theta}_t \right]_{x_1=l, x_2=-b}^{(2)} - \left[\int_{-b}^b \tau_{11}^{(3)} dx_2 \cdot \delta \phi^{(3)} \right]_{x_1=-l}^{(3)} \\
 & + \left[\int_{-b}^b \left(\tau_{13}^{(3)} + \tau_{12,2}^{(3)} \right) dx_2 \cdot \delta \hat{w} + \int_{-b}^b \left(\tau_{13}^{(3)} + \tau_{12,2}^{(3)} \right) x_2 dx_2 \cdot \delta \hat{\theta}_t \right]_{x_1=-l}^{(3)} + 2 \left[\tau_{12}^{(3)} \delta w^{(3)} \right]_{x_1=l, x_2=-b}^{(3)} \\
 & - \left[\tau_{12}^{(3)} \delta w^{(3)} + \tau_{12}^{(3)} \delta \hat{w} + \tau_{12}^{(3)} x_2 \cdot \delta \hat{\theta}_t \right]_{x_1=-l, x_2=-b}^{(3)} - \frac{M^{(1,2)}}{2} \left\{ \left[\left(\ddot{v} - 2\Omega \dot{\hat{u}}_r^{(0)} \right) \delta \hat{v} \right]_{x_2=\theta}^{(1)} \right. \\
 & \left. + \left[\left(\ddot{u}_2^{(0)} - 2\Omega \dot{\hat{w}} \right) \delta \hat{u}_2^{(0)} \right]_{x_1=-l}^{(2)} \right\} - \frac{J^{(1,2)}}{2} \left\{ \left[\left(\ddot{v} - \Omega \dot{\hat{\chi}} \right) \delta \hat{v} \right]_{x_2=\theta}^{(1)} + \left[\left(\ddot{\psi} - \Omega \dot{\hat{\phi}} \right) \delta \hat{\psi} \right]_{x_1=-l}^{(2)} \right\}
 \end{aligned}$$

$$\begin{aligned}
 & -\frac{{}^{(1,2)}J_t}{2} \left\{ \left[\begin{matrix} \ddot{\hat{g}}^{(1)} & \delta \hat{g}^{(1)} \end{matrix} \right]_{x_2=\theta}^{(1)} + \left[\begin{matrix} \ddot{\hat{\theta}}_t^{(2)} & \delta \hat{\theta}_t^{(2)} \end{matrix} \right]_{x_1=-l}^{(2)} \right\} - \frac{{}^{(2,3)}M}{2} \left\{ \left[\begin{matrix} \ddot{\hat{u}}_2^{(2)} - 2\Omega \dot{\hat{w}}^{(2)} & \delta \hat{u}_2^{(2)} \end{matrix} \right]_{x_1=l}^{(2)} \right. \\
 & \quad \left. + \left[\begin{matrix} \ddot{\hat{w}}^{(3)} + 2\Omega \dot{\hat{u}}_2^{(3)} & \delta \hat{w}^{(3)} \end{matrix} \right]_{x_1=-l}^{(3)} \right\} \\
 & - \frac{{}^{(2,3)}J}{2} \left\{ \left[\begin{matrix} \ddot{\hat{\psi}}^{(2)} - \Omega \dot{\hat{\phi}}^{(2)} & \delta \hat{\psi}^{(2)} \end{matrix} \right]_{x_1=l}^{(2)} + \left[\begin{matrix} \ddot{\hat{\phi}}^{(3)} + \Omega \dot{\hat{\psi}}^{(3)} & \delta \hat{\phi}^{(3)} \end{matrix} \right]_{x_1=-l}^{(3)} \right\} \\
 & - \frac{{}^{(2,3)}J_t}{2} \left\{ \left[\begin{matrix} \ddot{\hat{\theta}}_t^{(2)} & \delta \hat{\theta}_t^{(2)} \end{matrix} \right]_{x_1=l}^{(2)} + \left[\begin{matrix} \ddot{\hat{\theta}}_t^{(3)} & \delta \hat{\theta}_t^{(3)} \end{matrix} \right]_{x_1=-l}^{(3)} \right\} \\
 & + \delta \left[\frac{1}{2} \left[\int_{R_i}^{R_o} \left(\tau_{\theta z}^{(1)} + \tau_{\theta r,r}^{(1)} \right) dx_1 \right]_{x_2=\theta}^{(1)} + \left[\int_{-b}^b \tau_{12}^{(2)} dx_2 \right]_{x_1=-l}^{(2)} + \frac{{}^{(1,2)}M}{2} \left\{ \left[\begin{matrix} \ddot{\hat{v}}^{(1)} - 2\Omega \dot{\hat{u}}_r^{(1)} \end{matrix} \right]_{x_2=\theta}^{(1)} \right. \right. \\
 & \quad \left. \left. - \left[\begin{matrix} \ddot{\hat{u}}_2^{(2)} - 2\Omega \dot{\hat{w}}^{(2)} \end{matrix} \right]_{x_1=-l}^{(2)} \right\} \right] \left\{ \left[\begin{matrix} \hat{v}^{(1)} \end{matrix} \right]_{x_2=\theta}^{(1)} - \left[\begin{matrix} \hat{u}_2^{(2)} \end{matrix} \right]_{x_1=-l}^{(2)} \right\} - \delta \left[\frac{1}{2} \left[\int_{R_i}^{R_o} \tau_{\theta\theta}^{(1)} dx_1 \right]_{x_2=\theta}^{(1)} \right. \\
 & \quad \left. + \left[\int_{-b}^b \tau_{11}^{(2)} dx_2 \right]_{x_1=-l}^{(2)} \right] \\
 & - \frac{{}^{(1,2)}J}{2} \left\{ \left[\begin{matrix} \ddot{\hat{v}}^{(1)} - \Omega \dot{\hat{\chi}}^{(1)} \end{matrix} \right]_{x_2=\theta}^{(1)} - \left[\begin{matrix} \ddot{\hat{\psi}}^{(2)} - \Omega \dot{\hat{\phi}}^{(2)} \end{matrix} \right]_{x_1=-l}^{(2)} \right\} \left\{ \left[\begin{matrix} \hat{v}^{(1)} \end{matrix} \right]_{x_2=\theta}^{(1)} - \left[\begin{matrix} \hat{\psi}^{(2)} \end{matrix} \right]_{x_1=-l}^{(2)} \right\} \\
 & \quad + \delta \left[\frac{1}{2} \left[\left[\tau_{12}^{(2)} \right]_{x_1=-l, x_2=b}^{(2)} \right]_{x_1=-l, x_2=-b}^{(2)} \right] \\
 & + \left[\int_{R_i}^{R_o} \left(\tau_{\theta z}^{(1)} + \tau_{\theta r,r}^{(1)} \right) (r - r_0) dx_1 \right]_{x_2=\theta}^{(1)} - \left[\tau_{r\theta}^{(1)} (r - r_0) \right]_{x_1=R_o, x_2=\theta}^{(1)} \\
 & \quad - \left[\tau_{r\theta}^{(1)} (r - r_0) \right]_{x_1=R_i, x_2=\theta}^{(1)}
 \end{aligned}$$

$$\begin{aligned}
 & - \left[\int_{-b}^b \left(\tau_{13}^{(2)} + \tau_{12,2}^{(2)} \right) x_2 \, d x_2 \right]_{x_1=-l}^{(2)} \\
 & + \frac{J_t^{(1,2)}}{2} \left\{ \left[\begin{matrix} \hat{\phi}^{(1)} \\ \hat{\theta}_t^{(1)} \end{matrix} \right]_{x_2=\theta}^{(1)} + \left[\begin{matrix} \hat{\phi}^{(2)} \\ \hat{\theta}_t^{(2)} \end{matrix} \right]_{x_1=-l}^{(2)} \right\} \left\{ \left[\begin{matrix} \hat{\phi}^{(1)} \\ \hat{\theta}_t^{(1)} \end{matrix} \right]_{x_2=\theta}^{(1)} + \left[\begin{matrix} \hat{\phi}^{(2)} \\ \hat{\theta}_t^{(2)} \end{matrix} \right]_{x_1=-l}^{(2)} \right\} + \delta \left[\frac{1}{2} \left[\int_{-b}^b \tau_{12}^{(2)} \, d x_2 \right]_{x_1=l}^{(2)} \right. \\
 & + \left. \left[\int_{-b}^b \left(\tau_{13}^{(3)} + \tau_{12,2}^{(3)} \right) \, d x_2 \right]_{x_1=-l}^{(3)} + \frac{M^{(2,3)}}{2} \left\{ \left[\ddot{u}_2^{(2)} - 2\Omega \dot{w}^{(2)} \right]_{x_1=l}^{(2)} - \left[\dot{w}^{(3)} + 2\Omega \dot{u}_2^{(3)} \right]_{x_1=-l}^{(3)} \right\} \right] \\
 & \times \left\{ \left[\dot{u}_2^{(2)} \right]_{x_1=l}^{(2)} - \left[\dot{w}^{(3)} \right]_{x_1=-l}^{(3)} \right\} + \delta \left[-\frac{1}{2} \left[\int_{-b}^b \tau_{11}^{(2)} x_2 \, d x_2 \right]_{x_1=l}^{(2)} + \left[\int_{-b}^b \tau_{11}^{(3)} \, d x_2 \right]_{x_1=-l}^{(3)} \right. \\
 & - \left. \frac{J^{(2,3)}}{2} \left\{ \left[\dot{\psi}^{(2)} - \Omega \dot{\phi}^{(2)} \right]_{x_1=l}^{(2)} - \left[\dot{\phi}^{(3)} + \Omega \dot{\psi}^{(3)} \right]_{x_1=-l}^{(3)} \right\} \left\{ \left[\dot{\psi}^{(2)} \right]_{x_1=l}^{(2)} - \left[\dot{\phi}^{(3)} \right]_{x_1=-l}^{(3)} \right\} \right. \\
 & \left. + \delta \left[\frac{1}{2} \left[- \left[\tau_{12}^{(2)} x_2 \right]_{x_1=l, x_2=-b}^{(2)} \right]_{x_1=l, x_2=b}^{(2)} \right. \right. \\
 & \left. - \left[\tau_{12}^{(3)} x_2 \right]_{x_1=-l, x_2=-b}^{(3)} + \left[\int_{-b}^b \left(\tau_{13}^{(2)} + \tau_{12,2}^{(2)} \right) x_2 \, d x_2 \right]_{x_1=l}^{(2)} + \left[\int_{-b}^b \left(\tau_{13}^{(3)} + \tau_{12,2}^{(3)} \right) x_2 \, d x_2 \right]_{x_1=-l}^{(3)} \right. \\
 & \left. + \frac{J_t^{(2,3)}}{2} \left\{ \left[\begin{matrix} \hat{\theta}_t^{(2)} \\ \hat{\theta}_t^{(2)} \end{matrix} \right]_{x_1=l}^{(2)} - \left[\begin{matrix} \hat{\theta}_t^{(3)} \\ \hat{\theta}_t^{(3)} \end{matrix} \right]_{x_1=-l}^{(3)} \right\} \left\{ \left[\begin{matrix} \hat{\theta}_t^{(2)} \\ \hat{\theta}_t^{(2)} \end{matrix} \right]_{x_1=l}^{(2)} - \left[\begin{matrix} \hat{\theta}_t^{(3)} \\ \hat{\theta}_t^{(3)} \end{matrix} \right]_{x_1=-l}^{(3)} \right\} \right\} \right], \tag{7c}
 \end{aligned}$$

and for the sensing motion in the form

$$T_1^{RS} + T_2^{RS} + T_3^{RS} = 0, \tag{8}$$

where

$$\begin{aligned}
 T_1^{RS} \doteq & \int_{t_0}^t dt \left[\left[\int_S^{(1)} dS \left\{ \left(\tau_{rr,r}^{(0)} + \left\{ \tau_{r\theta,\theta}^{(0)} + \left(\tau_{rr}^{(0)} - \tau_{\theta\theta}^{(0)} \right) \right\} / r - 2\rho h \left(\ddot{u}_r^{(0)} + 2\Omega \sin \theta \dot{\tilde{v}} \right) \right) \delta u_r^{(0)} \right. \right. \\
 & + \left. \left(\tau_{\theta\theta,\theta}^{(0)} / r + \tau_{r\theta,r}^{(0)} + \frac{2}{r} \tau_{r\theta}^{(0)} - 2\rho h \left(\ddot{u}_\theta^{(0)} + 2\Omega \cos \theta \dot{\tilde{v}} \right) \right) \delta u_\theta^{(0)} \right\} \\
 & + \int_S^{(2)} dS \left\{ \left(\tau_{a3,a}^{(2)} - 2\rho h \left(\dot{w}^{(2)} + 2\Omega \dot{u}_2^{(2)} \right) \right) \delta w^{(2)} + \left(\tau_{ab,a}^{(2)} - \tau_{3b}^{(2)} \right) \delta u_b^{(2)} \right\} \\
 & + \int_S^{(2)} dS \left(\tau_{ab,a}^{(0)} - 2\rho h \dot{u}_b^{(0)} \right) \delta u_b^{(0)} \\
 & + \left. \int_S^{(3)} dS \left(\tau_{ab,a}^{(0)} - 2\rho h \left(\ddot{u}_b^{(0)} - 2\delta_{2b} \Omega \dot{w} \right) \right) \delta u_b^{(0)} \right] \right], \tag{9a}
 \end{aligned}$$

$$\begin{aligned}
 T_2^{RS} \doteq & \int_{t_0}^t dt \left[\left[- \int_{-\Theta}^{\Theta} dx_2 \left[r \left\{ \tau_{rr}^{(0)} \delta u_r^{(0)} + \tau_{r\theta}^{(0)} \delta u_\theta^{(0)} \right\} \right]_{x_1=R_i}^{(1)} \right. \right. \\
 & - \int_{-l}^l dx_1 \left[\left(\tau_{23}^{(2)} + \tau_{21,1}^{(2)} \right) \delta w^{(2)} - \tau_{22}^{(2)} \delta w_{,2}^{(2)} \right]_{x_2=b}^{(2)} - \int_{-l}^l dx_1 \left[\tau_{21}^{(2)} \delta u_1^{(2)} + \tau_{22}^{(2)} \delta u_2^{(2)} \right]_{x_2=-b}^{(2)} \\
 & - \left. \int_{-l}^l dx_1 \left[\tau_{21}^{(0)} \delta u_1^{(0)} + \tau_{22}^{(0)} \delta u_2^{(0)} \right]_{x_2=-b}^{(3)} \right] \right], \tag{9b}
 \end{aligned}$$

$$\begin{aligned}
 T_3^{RS} \doteq & \int_{t_0}^t dt \left[\left[- \left[\int_{R_i}^{R_o} \tau_{\theta r}^{(0)} dx_1 \cdot \delta \hat{u}_r^{(0)} - \int_{R_i}^{R_o} \tau_{\theta\theta}^{(0)} (r - r_0) dx_1 \cdot \delta \hat{\chi} + \int_{R_i}^{R_o} \tau_{\theta\theta}^{(0)} dx_1 \cdot \delta \hat{u}_\theta^{(0)} \right]_{x_2=\Theta}^{(1)} \right. \right. \\
 & - \left. \int_{R_i}^{R_o} dx_1 \left[u_r^{(0)} \delta \tau_{\theta r}^{(0)} + u_\theta^{(0)} \delta \tau_{\theta\theta}^{(0)} \right]_{x_2=-\Theta}^{(1)} - \left[\int_{-b}^b \left(\tau_{13}^{(2)} + \tau_{12,2}^{(2)} \right) dx_2 \cdot \delta \hat{w} - \int_{-b}^b \tau_{11}^{(2)} dx_2 \cdot \delta \hat{\phi} \right]_{x_1=-l}^{(2)} \right] \right],
 \end{aligned}$$

$$\begin{aligned}
 & - \left[\tau_{12}^{(1)} \delta \dot{w}^{(2)} + \tau_{12}^{(2)} \delta \dot{w}^{(2)} \right]_{x_1=-l, x_2=b}^{(2)} + \left[\tau_{12}^{(1)} \delta \dot{w}^{(2)} + \tau_{12}^{(2)} \delta \dot{w}^{(2)} \right]_{x_1=l, x_2=-b}^{(2)} \\
 & - \int_{-b}^b dx_2 \left[\int_{-b}^b \tau_{11}^{(2)} dx_2 \cdot \delta \hat{u}_1^{(2)} \right]_{x_1=-l}^{(2)} - \int_{-b}^b dx_2 \left[\tau_{11}^{(3)} \delta u_1^{(3)} + \tau_{12}^{(3)} \delta u_2^{(3)} \right]_{x_1=l}^{(3)} \\
 & + \left[\int_{-b}^b \tau_{11}^{(3)} dx_2 \cdot \hat{u}_1^{(3)} - \int_{-b}^b \tau_{11}^{(3)} x_2 dx_2 \cdot \delta \hat{\psi} + \int_{-b}^b \tau_{12}^{(3)} dx_2 \cdot \delta \hat{u}_2^{(3)} \right]_{x_1=-l}^{(3)} \\
 & - \frac{M^{(1,2)}}{2} \left\{ \left[\ddot{u}_\theta^{(1)} \delta \hat{u}_\theta^{(1)} + \left(\ddot{u}_r^{(1)} + 2\Omega \dot{\hat{v}} \right) \delta \hat{u}_r^{(1)} \right]_{x_2=\theta}^{(1)} + \left[\ddot{u}_1^{(2)} \delta \hat{u}_1^{(2)} + \left(\ddot{w} + 2\Omega \dot{\hat{u}}_2^{(2)} \right) \delta \hat{w} \right]_{x_1=-l}^{(2)} \right\} \\
 & - \frac{M^{(2,3)}}{2} \left\{ \left[\ddot{u}_1^{(2)} \delta \hat{u}_1^{(2)} + \left(\ddot{w} + 2\Omega \dot{\hat{u}}_2^{(2)} \right) \delta \hat{w} \right]_{x_1=l}^{(2)} + \left[\ddot{u}_1^{(3)} \delta \hat{u}_1^{(3)} + \left(\ddot{u}_2^{(3)} - 2\Omega \dot{\hat{w}} \right) \delta \hat{u}_2^{(3)} \right]_{x_1=-l}^{(3)} \right\} \\
 & - \frac{J^{(1,2)}}{2} \left\{ \left[\left(\dot{\hat{\chi}} + \Omega \dot{\hat{v}} \right) \delta \hat{\chi} \right]_{x_2=\theta}^{(1)} + \left[\left(\dot{\hat{\phi}} + \Omega \dot{\hat{\psi}} \right) \delta \hat{\phi} \right]_{x_1=-l}^{(2)} \right\} - \frac{J^{(2,3)}}{2} \left\{ \left[\left(\dot{\hat{\phi}} + \Omega \dot{\hat{\psi}} \right) \delta \hat{\phi} \right]_{x_1=l}^{(2)} \right. \\
 & \left. + \left[\left(\dot{\hat{\psi}} - \Omega \dot{\hat{\phi}} \right) \delta \hat{\psi} \right]_{x_1=-l}^{(3)} \right\} + \delta \left[\frac{1}{2} \left[\int_{R_i}^{R_o} \tau_{\theta r}^{(1)} dx_1 \right]_{x_2=\theta}^{(1)} + \left[\int_{-b}^b \left(\tau_{13}^{(2)} + \tau_{12,2}^{(2)} \right) dx_2 \right]_{x_1=-l}^{(2)} \right. \\
 & \left. + \frac{M^{(1,2)}}{2} \left\{ \left[\ddot{u}_r^{(1)} + 2\Omega \dot{\hat{v}} \right]_{x_2=\theta}^{(1)} - \left[\ddot{w} + 2\Omega \dot{\hat{u}}_2^{(2)} \right]_{x_1=-l}^{(2)} \right\} \right\} \left\{ \left[\hat{u}_r^{(1)} \right]_{x_2=\theta}^{(1)} - \left[\hat{w} \right]_{x_1=-l}^{(2)} \right\} \\
 & + \delta \left[\frac{1}{2} \left[- \left[\int_{R_i}^{R_o} \tau_{\theta\theta}^{(1)} (r - r_0) dx_1 \right]_{x_2=\theta}^{(1)} - \left[\int_{-b}^b \tau_{11}^{(2)} dx_2 \right]_{x_1=-l}^{(2)} \right. \right.
 \end{aligned}$$

$$\begin{aligned}
 & + \frac{J^{(1,2)}}{2} \left\{ \left[\begin{matrix} \ddot{\chi}^{(1)} + \Omega \dot{\delta}^{(1)} \\ \ddot{\phi}^{(2)} + \Omega \dot{\psi}^{(2)} \end{matrix} \right]_{x_2=\theta}^{(1)} - \left[\begin{matrix} \ddot{\phi}^{(2)} + \Omega \dot{\psi}^{(2)} \\ \ddot{\chi}^{(1)} + \Omega \dot{\delta}^{(1)} \end{matrix} \right]_{x_1=-l}^{(2)} \right\} \\
 & \times \left\{ \left[\begin{matrix} \dot{\chi}^{(1)} \\ \dot{\phi}^{(2)} \end{matrix} \right]_{x_2=\theta}^{(1)} - \left[\begin{matrix} \dot{\phi}^{(2)} \\ \dot{\chi}^{(1)} \end{matrix} \right]_{x_1=-l}^{(2)} \right\} + \delta \left[\frac{1}{2} \left[- \int_{R_i}^{R_o} \tau_{\theta\theta}^{(0)} d x_1 \right]_{x_2=\theta}^{(1)} + \left[\int_{-b}^b \tau_{11}^{(0)} d x_2 \right]_{x_1=-l}^{(2)} \right. \\
 & + \frac{M^{(1,2)}}{2} \left\{ \left[\begin{matrix} \ddot{u}_\theta^{(0)} \\ \ddot{u}_1^{(0)} \end{matrix} \right]_{x_2=\theta}^{(1)} - \left[\begin{matrix} \ddot{u}_1^{(0)} \\ \ddot{u}_\theta^{(0)} \end{matrix} \right]_{x_1=-l}^{(2)} \right\} \left\{ \left[\begin{matrix} \dot{u}_\theta^{(0)} \\ \dot{u}_1^{(0)} \end{matrix} \right]_{x_2=\theta}^{(1)} - \left[\begin{matrix} \dot{u}_1^{(0)} \\ \dot{u}_\theta^{(0)} \end{matrix} \right]_{x_1=-l}^{(2)} \right\} \\
 & + \delta \left[\frac{1}{2} \left[\left[\int_{-b}^b \tau_{11}^{(0)} d x_2 \right]_{x_1=l}^{(2)} + \left[\int_{-b}^b \tau_{11}^{(0)} d x_2 \right]_{x_1=-l}^{(3)} \right. \right. \\
 & + \frac{M^{(2,3)}}{2} \left\{ \left[\begin{matrix} \ddot{u}_1^{(0)} \\ \ddot{u}_1^{(0)} \end{matrix} \right]_{x_1=l}^{(2)} - \left[\begin{matrix} \ddot{u}_1^{(0)} \\ \ddot{u}_1^{(0)} \end{matrix} \right]_{x_1=-l}^{(3)} \right\} \left\{ \left[\begin{matrix} \dot{u}_1^{(0)} \\ \dot{u}_1^{(0)} \end{matrix} \right]_{x_1=l}^{(2)} - \left[\begin{matrix} \dot{u}_1^{(0)} \\ \dot{u}_1^{(0)} \end{matrix} \right]_{x_1=-l}^{(3)} \right\} \\
 & + \delta \left[\frac{1}{2} \left[\left[\int_{-b}^b \left(\tau_{13}^{(0)} + \tau_{12,2}^{(1)} \right) d x_2 \right]_{x_1=l}^{(2)} \right. \right. \\
 & - \left[\int_{-b}^b \tau_{12}^{(0)} d x_2 \right]_{x_1=-l}^{(3)} + \frac{M^{(2,3)}}{2} \left\{ \left[\begin{matrix} \ddot{w}^{(2)} + 2\Omega \dot{u}_2^{(0)} \\ \ddot{u}_2^{(0)} - 2\Omega \dot{w}^{(3)} \end{matrix} \right]_{x_1=l}^{(2)} + \left[\begin{matrix} \ddot{u}_2^{(0)} - 2\Omega \dot{w}^{(3)} \\ \ddot{w}^{(3)} + 2\Omega \dot{u}_2^{(0)} \end{matrix} \right]_{x_1=-l}^{(3)} \right\} \\
 & \times \left\{ \left[\begin{matrix} \dot{w}^{(2)} \\ \dot{u}_2^{(0)} \end{matrix} \right]_{x_1=l}^{(2)} + \left[\begin{matrix} \dot{u}_2^{(0)} \\ \dot{w}^{(3)} \end{matrix} \right]_{x_1=-l}^{(3)} \right\} + \delta \left[\frac{1}{2} \left[- \left[\int_{-b}^b \tau_{11}^{(1)} d x_2 \right]_{x_1=l}^{(2)} + \left[\int_{-b}^b \tau_{11}^{(0)} x_2 d x_2 \right]_{x_1=-l}^{(3)} \right. \right. \\
 & + \frac{J^{(2,3)}}{2} \left\{ \left[\begin{matrix} \ddot{\phi}^{(2)} + \Omega \dot{\psi}^{(2)} \\ \ddot{\psi}^{(3)} - \Omega \dot{\phi}^{(3)} \end{matrix} \right]_{x_1=l}^{(2)} + \left[\begin{matrix} \ddot{\psi}^{(3)} - \Omega \dot{\phi}^{(3)} \\ \ddot{\phi}^{(2)} + \Omega \dot{\psi}^{(2)} \end{matrix} \right]_{x_1=-l}^{(3)} \right\} \left\{ \left[\begin{matrix} \dot{\phi}^{(2)} \\ \dot{\psi}^{(3)} \end{matrix} \right]_{x_1=l}^{(2)} + \left[\begin{matrix} \dot{\psi}^{(3)} \\ \dot{\phi}^{(2)} \end{matrix} \right]_{x_1=-l}^{(3)} \right\} \Bigg], \tag{9c}
 \end{aligned}$$

where the tilde (\sim) is used to represent the terms related to the Coriolis forces and the gyroscopic moments, which are treated as d'Alembertian inertial forces and moments in this work.

2.2. Forced vibration analysis for the actuating motion of the gyroscope

As noted in Ref. [3], the problem of the free flexural vibrations of a plate with two opposite edges free and the other edges constrained arbitrarily cannot be solved exactly. In this work we treat this problem by first obtaining the exact solutions for low frequency flexural waves in plates with two opposite edges free. These solutions result in three sets of dispersion curves for wavenumbers in the x_2 , x_1 and x_1 directions, respectively, in which we take the three sets of differential equations from the homogeneous portions of the variational equation (6). Since the configuration is such that the voltage drives the motion in the actuating direction and the superposed angular velocity causes motion in the sensing direction and the angular velocity satisfies the condition $|\Omega| \ll \omega$, the sensing motion may be ignored in the forcing of the actuator.

Hence, the displacements orthogonal to the actuator motion, i.e., $\tilde{u}_r^{(0)}$, $\tilde{u}_\theta^{(0)}$, $\tilde{w}^{(2)}$, $\tilde{u}_1^{(3)}$, $\tilde{u}_2^{(3)}$, are taken to vanish in this section. In the homogeneous case from Eqs. (10), (11a), (11b), (51)–(53) of Ref. [1], and in accordance with Eqs. (21) and (13), (19) and (23) of Ref. [4], the differential equation and two conditions at the two free opposing edges of the annular sector plate in flexural vibration can be represented in the form

$$\frac{1}{r^2} \left(r^2 v_{,rrr} \right)_{,r} + \frac{2}{r^2} \left(v_{,r} - \frac{v}{r} \right)_{,r\theta\theta} + \frac{1}{r} \left\{ \frac{1}{r^3} \left(v_{,\theta\theta} + 2 \frac{v}{r} \right)_{,\theta\theta} - \left(\frac{1}{r} v_{,r} \right)_{,r} \right\} - \hat{\kappa}^2 \omega^2 v = 0, \tag{10}$$

$$v_{,rr} + \frac{\tilde{\nu}}{r} \left(v_{,r} + \frac{1}{r} v_{,\theta\theta} \right) = 0, \quad v_{,rrr} - \frac{v_{,r}}{r^2} + \frac{v_{,rr}}{r} - \frac{v_{,\theta\theta}}{r^3} + \frac{(2 - \tilde{\nu})}{r^2} \left(v_{,r\theta\theta} - \frac{v_{,\theta\theta}}{r} \right) = 0, \tag{11}$$

where $\hat{\kappa} \doteq \sqrt{2\rho h / \tilde{D}}$.

From Eqs. (10), (11a), (11b), (55) and (56) of Ref. [1] and in accordance with Eqs. (8), (9) and (7), (3)₂ and (4) of Ref. [5], we obtain the differential equations and the two conditions at the two free opposing edges of the rectangular plate in plane stress in the form

$$c_{11}^{E*} u_{1,11}^{(2)} + \left(c_{12}^{E*} + c_{66} \right) u_{2,12}^{(2)} + c_{66} u_{1,11}^{(2)} + \rho \omega^2 u_1^{(2)} = 0, \tag{12a}$$

$$\left(c_{12}^{E*} + c_{66} \right) u_{1,12}^{(2)} + c_{11}^{E*} u_{2,22}^{(2)} + c_{66} u_{2,11}^{(2)} + \rho \omega^2 u_2^{(2)} = 0, \tag{12b}$$

$$u_{2,2}^{(2)} + \hat{\nu} u_{1,1}^{(2)} = 0, \quad u_{1,2}^{(2)} + u_{2,1}^{(2)} = 0, \tag{13}$$

and from Eqs. (10), (11a), (11b), (46a), (46b) and (50)₂ of Ref. [1] and in accordance with Eqs. (29) and (31), (32) with (21)₂ and (23)₂ of Ref. [3], we obtain the differential equation and the two free edge conditions [with $V_A = 0$ in Eq. (6)] of the rectangular plate in flexural motion in the form

$${}^{(m)}w_{,1111} + 2 {}^{(m)}w_{,1122} + {}^{(m)}w_{,2222} - \bar{\kappa}^2 \omega^2 {}^{(m)}w = 0, \tag{14}$$

$${}^{(m)}w_{,22} + \bar{\nu} {}^{(m)}w_{,11} = 0, \quad {}^{(m)}w_{,222} + (2 - \bar{\nu}) {}^{(m)}w_{,211} = 0, \quad m = 1, 2. \tag{15}$$

Following the procedures explained in Sections 3 of Refs. [3–5], we obtain the solution, which yields three sets of dispersion relations for the out-of-plane motion of the annular sector plate, in-plane and out-of-plane motions of the rectangular plates in the homogeneous case, i.e., when the driving voltage V_A vanishes. In the inhomogeneous case, i.e., when $V_A \neq 0$ and $V_A = \bar{V}_A e^{i\omega t}$, we take a relatively small number of these waves at a given frequency to satisfy the inhomogeneous variational equation¹ in Eq. (6).

According to Eq. (44) of Ref. [4], Eqs. (37) and (38) of Ref. [5] and Eq. (51) of Ref. [3], the solution functions may be written in the form

$${}^{(1)}v = \sum_{p=1}^{P^{(A)}} \sum_{q=1}^4 \sum_{n=1}^2 C_{pqn}^{(A)} \bar{H}_{pq}^{(A)} G_{pq}^{(A)}(r) \sin \left\{ i_p^{(A)} \theta + (n-1)\pi/2 \right\} e^{i\omega t}, \tag{16}$$

$${}^{(2)}u_1^{(0)} = \sum_{p=1}^{P_1^{(A)}} \sum_{q=1}^2 \sum_{n=1}^2 B_{pqn}^{(A,A)} \bar{H}_{1pq}^{(A,A)} \sin \left(\zeta_{pq}^{(A,A)} x_2 \right) \cos \left(\gamma_p^{(A,A)} x_1 + (n-1)\pi/2 \right) e^{i\omega t}, \tag{17a}$$

$${}^{(2)}u_2^{(0)} = \sum_{p=1}^{P_1^{(A)}} \sum_{q=1}^2 \sum_{n=1}^2 B_{pqn}^{(A,A)} \bar{H}_{2pq}^{(A,A)} \cos \left(\zeta_{pq}^{(A,A)} x_2 \right) \sin \left(\gamma_p^{(A,A)} x_1 + (n-1)\pi/2 \right) e^{i\omega t}, \tag{17b}$$

$${}^{(2)}w = \sum_{p=1}^{P_2^{(A)}} \sum_{q=1}^2 \sum_{n=1}^2 A_{pn}^{(A,A)} \bar{H}_{pq}^{(A,A)} \sin \left\{ \eta_{pq}^{(A,A)} x_2 \right\} \sin \left\{ \zeta_p^{(A,A)} x_1 + (n-1)\pi/2 \right\} e^{i\omega t}, \tag{17c}$$

¹See footnote 6 contained in Part 1 of this work [1].

$$\begin{aligned}
 w^{(3)} = & \sum_{p=1}^{P_1^{(3)}} \sum_{q=1}^2 \sum_{n=1}^2 A_{pqn}^{(A,S)} \overline{H}_{pq}^{(A,S)} \cos \left\{ \eta_{pq}^{(A,S)} x_2 \right\} \sin \left\{ \zeta_p^{(A,S)} x_1 + (n-1)\pi/2 \right\} e^{i\omega t} \\
 & + \sum_{p=1}^{P_2^{(3)}} \sum_{q=1}^2 \sum_{n=1}^2 A_{pn}^{(A,A)} \overline{H}_{pq}^{(A,A)} \sin \left\{ \eta_{pq}^{(A,A)} x_2 \right\} \sin \left\{ \zeta_p^{(A,A)} x_1 + (n-1)\pi/2 \right\} e^{i\omega t}, \quad (18)
 \end{aligned}$$

where $P_k^{(A)}, P_k^{(A)}, k = 1, 2, m = 2, 3$ are the numbers of dispersion curves taken, $C_{pqn}^{(A)}, B_{pqn}^{(A,A)}, A_{pn}^{(A,A)}, A_{pqn}^{(A,S)}, A_{pn}^{(A,A)}$ are unknown amplitudes to be determined (see footnote 1), $\overline{H}_{pq}^{(A)}, \overline{H}_{1pq}^{(A,A)}, \overline{H}_{2pq}^{(A,A)}$,

$\overline{H}_{pq}^{(A,A)}, \overline{H}_{pq}^{(A,S)}, \overline{H}_{pq}^{(A,A)}$ are amplitude ratios determined from the solutions of the homogeneous

differential equations, $\nu_p^{(A)}, \gamma_p^{(A,A)}, \zeta_p^{(A,A)}, \zeta_p^{(A,S)}, \varsigma_{pq}^{(A,A)}, \eta_{pq}^{(A,A)}$ and $\eta_{pq}^{(A,S)}$ are wavenumbers, and $G_{pq}^{(A)}(r)$

is a series-type solution with radial functional dependence as defined in Eq. (32) of Ref. [4]. All quantities appearing in Eqs. (16)–(18) are explained in detail in Sections 3 and 4 of Refs. [3–5]. It should be noted that $w^{(2)}$ in Eq. (17c) and the second term in Eq. (18) are required in the description

of the actuator because $v^{(1)}$ in the annular sector plate contains this motion through the power

series term $G_{pq}^{(A)}(r)$. In Eq. (16)–(18), the symbol A in the first place of the superscript represents the actuator and A, S in the second place, respectively, represent the antisymmetric and symmetric modes, if they exist. It should be noted that all the amplitudes, $C_{pqn}^{(A)}, B_{pqn}^{(A,A)}, A_{pqn}^{(A,S)}$ in Eqs. (16),

(17a), (17b) and the first term of Eq. (18),² must be determined from the linear algebra obtained from the variational equation that contains inhomogeneous edge and interface conditions, in accordance with footnote 1. The solution of the inhomogeneous linear algebraic equations yields the values of the unknown amplitudes and thus the solution for the vibration in the actuating direction.

Since the foregoing analysis is completely non-dissipative, at resonance, which is of primary interest in this work, the amplitude of vibration would become unbounded. Inasmuch as no real material is actually non-dissipative, this never happens. However, when the damping is not great, the self-adjoint description yields the resonant frequencies and everything else except the amplitudes with great accuracy in the case of steady-state vibrations. Furthermore, in the lightly damped case the actual details of the damping are irrelevant in the description. Under such circumstances all that need be done is to replace the real driving frequency by the complex

²No inhomogeneous term occurs in the variational equation associated with the second term in (18).

quantity

$$\omega \left(1 - \frac{i}{2Q} \right), \tag{19}$$

where Q is called the quality factor,³ in the calculation of the amplitudes in the inhomogeneous case, and then take the real part of the solution.

2.3. Forced vibration analysis for the sensing motion of the gyroscope

Although in the case of the actuator all inhomogeneous terms occurred only in the edge conditions and not in the differential equations, in the case of the sensor inhomogeneous terms occur in the differential equations as well as the edge conditions. Consequently in this work, we employ a solution procedure whereby we transfer the inhomogeneous terms from the differential equations into the edge conditions [6]. In order to do this we write the solution as an auxiliary plus a residual part and select the auxiliary part to be particular solutions of the inhomogeneous equations in order that the residual part satisfies homogeneous differential equations. To this end,

we choose the auxiliary functions $u_r^{(0)}$, $u_\theta^{(0)}$, $w^{(2)}$, $u_1^{(3)}$ and $u_2^{(3)}$ to be particular solutions of the differential equations

$$\begin{aligned} & c_{11}^{E*} \left(u_{r,rr}^{(1)A} + \frac{u_{r,r}^{(0)}}{r} - \frac{u_r^{(0)}}{r^2} \right) + \frac{c_{66}^{(1)A} u_{r,\theta\theta}^{(0)}}{r^2} + \frac{(c_{12}^{E*} + c_{66}) u_{\theta,r\theta}^{(1)A}}{r} - \frac{(c_{11}^{E*} + c_{66}) u_{\theta,\theta}^{(0)}}{r^2} + \rho \omega^2 u_r^{(1)A} \\ & = 2\rho i\omega \Omega \sin \theta \cdot \tilde{v}^{(1)}, \end{aligned} \tag{20a}$$

$$\begin{aligned} & \frac{(c_{12}^{E*} + c_{66}) u_{r,r\theta}^{(1)A}}{r} + \frac{(c_{11}^{E*} + c_{66}) u_{r,\theta}^{(1)A}}{r^2} + \frac{c_{11}^{E*} u_{\theta,\theta\theta}^{(1)A}}{r^2} + c_{66} \left(u_{\theta,rr}^{(1)A} + \frac{u_{\theta,r}^{(0)}}{r} - \frac{u_\theta^{(0)}}{r^2} \right) + \rho \omega^2 u_\theta^{(1)A} \\ & = 2\rho i\omega \Omega \cos \theta \cdot \tilde{v}^{(1)}, \end{aligned} \tag{20b}$$

$$w_{,1111}^{(2)A} + 2 w_{,1122}^{(2)A} + w_{,2222}^{(2)A} - \hat{\kappa}^2 \omega^2 w^{(2)A} = -2\hat{\kappa}^2 i\omega \Omega \dot{u}_2^{(0)}, \tag{21}$$

$$c_{11}^{E*} u_{1,11}^{(3)A} + (c_{12}^{E*} + c_{66}) u_{2,12}^{(3)A} + c_{66} u_{1,11}^{(0)} + \rho \omega^2 u_1^{(0)} = 0, \tag{22a}$$

³ Larger values of Q give sharper peaked responses and smaller values of Q give flatter or more broadened responses.

$$\left(c_{12}^{E*} + c_{66} \right) u_{1,12}^{(3)A} + c_{11}^{E*} u_{2,22}^{(3)A} + c_{66} u_{2,11}^{(3)A} + \rho \omega^2 u_2^{(3)A} = -2\rho i \omega \Omega \dot{w}^{(3)} \tag{22b}$$

without regard to edge conditions. Then inserting Eqs. (20)–(22) in the differential equation parts (8), which are given by T_1^{RS} in Eq. (9a), we find that the residual problem satisfies the homogeneous equations

$$c_{11}^{E*} \left(u_{r,rr}^{(1)R} + \frac{u_{r,r}^{(0)}}{r} - \frac{u_r^{(0)}}{r^2} \right) + \frac{c_{66} u_{r,\theta\theta}^{(0)}}{r^2} + \frac{\left(c_{12}^{E*} + c_{66} \right) u_{\theta,r\theta}^{(0)}}{r} - \frac{\left(c_{11}^{E*} + c_{66} \right) u_{\theta,\theta}^{(0)}}{r^2} + \rho \omega^2 u_r^{(0)} = 0, \tag{23a}$$

$$\frac{\left(c_{12}^{E*} + c_{66} \right) u_{r,r\theta}^{(0)}}{r} + \frac{\left(c_{11}^{E*} + c_{66} \right) u_{r,\theta}^{(0)}}{r^2} + \frac{c_{11}^{E*} u_{\theta,\theta\theta}^{(0)}}{r^2} + c_{66} \left(u_{\theta,rr}^{(0)} + \frac{u_{\theta,r}^{(0)}}{r} - \frac{u_{\theta}^{(0)}}{r^2} \right) + \rho \omega^2 u_{\theta}^{(0)} = 0, \tag{23b}$$

$$w_{,1111}^{(2)R} + 2 w_{,1122}^{(2)R} + w_{,2222}^{(2)R} - \hat{\kappa}^2 \omega^2 w^{(2)R} = 0, \tag{24a}$$

$$c_{11}^{E*} u_{1,11}^{(2)R} + \left(c_{12}^{E*} + c_{66} \right) u_{2,12}^{(2)R} + c_{66} u_{1,11}^{(0)} + \rho \omega^2 u_1^{(0)} = 0, \tag{24b}$$

$$\left(c_{12}^{E*} + c_{66} \right) u_{1,12}^{(0)} + c_{11}^{E*} u_{2,22}^{(0)} + c_{66} u_{2,11}^{(0)} + \rho \omega^2 u_2^{(0)} = 0, \tag{24c}$$

$$c_{11}^{E*} u_{1,11}^{(3)R} + \left(c_{12}^{E*} + c_{66} \right) u_{2,12}^{(0)} + c_{66} u_{1,11}^{(0)} + \rho \omega^2 u_1^{(0)} = 0, \tag{25a}$$

$$\left(c_{12}^{E*} + c_{66} \right) u_{1,12}^{(0)} + c_{11}^{E*} u_{2,22}^{(0)} + c_{66} u_{2,11}^{(0)} + \rho \omega^2 u_2^{(0)} = 0, \tag{25b}$$

which causes all integrations over areas to vanish in Eq. (8) through T_1^{RS} , and produces additional inhomogeneities in T_2^{RS} and T_3^{RS} in Eq. (9b) and (9c), which appear in Eq. (8). The substitution of

$$u_r^{(1)} = u_r^{(0)} + u_r^{(1)A}, \quad u_{\theta}^{(1)} = u_{\theta}^{(0)} + u_{\theta}^{(1)A}, \quad w = w^{(2)} + w^{(2)A}, \quad u_1^{(2)} = u_1^{(0)}, \quad u_2^{(2)} = u_2^{(0)}, \quad u_1^{(3)} = u_1^{(0)} + u_1^{(3)A} \quad \text{and}$$

$$u_2^{(3)} = u_2^{(0)} + u_2^{(3)A} \quad \text{into what remains in the variational equation (8), i.e., } T_2^{RS} + T_3^{RS} = 0, \text{ yields a}$$

set of linear inhomogeneous equations in the same number of unknown amplitudes as the equations.

Eqs. (20)–(22) show that the inhomogeneous forcing terms contain the rotation-rate Ω and the actuator velocity field. Since in the rectangular sections of the device the auxiliary solution is easily obtained simply by taking terms proportional to each actuator term in the equations and solving a simple algebraic equation for each amplitude, we do not present any detail here. However, in the case of the annular sector plate some detail should be presented because the actuator solution is given in terms of power series in r multiplying trigonometric functions of θ and a trigonometric function of θ is in each inhomogeneous term. From Eqs. (20a) and (20b) and the fact that the out-of-plane motion of the annular sector plate has displacement functions in the form

$$\tilde{v}^{(1)} = \sum_{p=1}^{P^{(A)}} \sum_{q=1}^4 \sum_{n=1}^2 \tilde{C}_{pqn}^{(A)} \overline{H}_{pq}^{(A)} G_{pq}^{(A)}(r) \sin \left\{ i_p^{(A)} \theta + (n-1)\pi/2 \right\} e^{i\omega t}, \tag{26}$$

the forcing functions, which are the terms on the right-hand side of Eqs. (20a) and (20b), are given by

$$2\rho i\omega \Omega \sin \theta \cdot \tilde{v}^{(1)} = \rho i\omega \Omega \sum_{p=1}^{P^{(A)}} \sum_{q=1}^4 \sum_{n=1}^2 \sum_{k=1}^2 \tilde{C}_{pqn}^{(A)} \overline{H}_{pq}^{(A)} G_{pq}^{(A)}(r) (-1)^k \sin \left(\Lambda_{pk}^{(1)} \theta + \frac{n\pi}{2} \right), \tag{27a}$$

$$2\rho i\omega \Omega \cos \theta \cdot \tilde{v}^{(1)} = -\rho i\omega \Omega \sum_{p=1}^{P^{(A)}} \sum_{q=1}^4 \sum_{n=1}^2 \sum_{k=1}^2 \tilde{C}_{pqn}^{(A)} \overline{H}_{pq}^{(A)} G_{pq}^{(A)}(r) \cos \left(\Lambda_{pk}^{(1)} \theta + \frac{n\pi}{2} \right), \tag{27b}$$

where

$$\Lambda_{pk}^{(1)} \doteq i_p^{(A)} - (-1)^k, \tag{28}$$

on account of the addition theorem for products of trigonometric functions.

The function $G_{pq}^{(A)}(r)$ in Eqs. (27a) and (27b) is a series-type function expanded about r_0 in the form (see Eq. (32) of Ref. [4])

$$G_{pq}^{(A)} = \sum_{m=0}^M \tilde{\alpha}_m^{(q)}(\xi_p^{(A)}) (r - r_0)^{\lambda_{(q)} + m}, \lambda_{(q)} = 0, 1, 2, 3 \text{ for } q = 1, \dots, 4, \tag{29}$$

where the $\tilde{\alpha}_m^{(q)}(\xi_p^{(A)})$ are known from the recursion equations obtained with the solution. We now write the solution functions of Eqs. (20a) and (20b) in the form

$$u_r^{(1)A} = \sum_{p=1}^{P^{(A)}} \sum_{q=1}^4 \sum_{n=1}^2 \sum_{k=1}^2 \Phi_{pqnk}^{(1)}(r) \sin \left(\Lambda_{pk}^{(1)} \theta + \frac{n\pi}{2} \right), \tag{30a}$$

$$u_{\theta}^{(0)} = \sum_{p=1}^{(1)A} \sum_{q=1}^4 \sum_{n=1}^2 \sum_{k=1}^2 \Psi_{pqnk}^{(1)}(r) \cos\left(\Lambda_{pk}^{(1)} \theta + \frac{n\pi}{2}\right), \tag{30b}$$

where we have introduced the definitions

$$\Phi_{pqnk}^{(1)} = \sum_{m=0}^M a_{pnkm}^{(q)} (r - r_0)^{\lambda_{(q)}+m}, \quad \Psi_{pqnk}^{(1)} = \sum_{m=0}^M b_{pnkm}^{(q)} (r - r_0)^{\lambda_{(q)}+m}. \tag{31}$$

The insertion of Eqs. (27a), (27b), (30a), (30b) and (31) in Eqs. (20a) and (20b), and the comparison of like powers of $(r - r_0)$ yields the coefficients $a_{pnkm}^{(q)}$ and $b_{pnkm}^{(q)}$ in terms of the known coefficients, which gives the auxiliary solution for the annular sector plate. As noted earlier at the beginning of Section 2.2, the problems of the free vibrations of plates with two opposite edges free and the other edges constrained arbitrarily cannot be solved exactly. Consequently, we proceed as in Section 2.2. To this end, we first note that from Eqs. (16), (17a), (17b), (57) and (58) of Ref. [1] and Eqs. (15)–(18) of Ref. [7], the differential equations and two conditions at the two free opposing edges of the annular sector plate in plane stress can be represented in the form

$$c_{11}^{E*} \left(u_{r,rr}^{(0)} + \frac{u_{r,r}^{(0)}}{r} - \frac{u_r^{(0)}}{r^2} \right) + \frac{c_{66} u_{r,\theta\theta}^{(0)}}{r^2} + \frac{(c_{12}^{E*} + c_{66}) u_{\theta,r\theta}^{(0)}}{r} - \frac{(c_{11}^{E*} + c_{66}) u_{\theta,\theta}^{(0)}}{r^2} + \rho\omega^2 u_r^{(0)} = 0, \tag{32a}$$

$$\frac{(c_{12}^{E*} + c_{66}) u_{r,r\theta}^{(0)}}{r} + \frac{(c_{11}^{E*} + c_{66}) u_{r,\theta}^{(0)}}{r^2} + \frac{c_{11}^{E*} u_{\theta,\theta\theta}^{(0)}}{r^2} + c_{66} \left(u_{\theta,rr}^{(0)} + \frac{u_{\theta,r}^{(0)}}{r} - \frac{u_{\theta}^{(0)}}{r^2} \right) + \rho\omega^2 u_{\theta}^{(0)} = 0, \tag{32b}$$

$$u_{r,r}^{(0)} + \frac{\hat{v}}{r} \left(u_{\theta,\theta}^{(0)} + u_r^{(0)} \right) = 0, \quad \frac{u_{r,\theta}^{(0)}}{r} + r \left(\frac{u_{\theta}^{(0)}}{r} \right)_{,r} = 0. \tag{33}$$

The procedures for the out-of-plane and in-plane motions of the rectangular plates, which are for the elements $V^{(2)}$ and $V^{(3)}$ of the sensor system, have been explained in Section 2.2 in the homogeneous case. In the inhomogeneous case, i.e., when $\Omega \neq 0$, we take a relatively small number of these waves at a given frequency to satisfy the inhomogeneous variational equation (see footnote 1) in Eq. (8).

According to Eqs. (49) and (50) of Ref. [7], Eq. (51) of Ref. [3], and Eqs. (37) and (38) of Ref. [5], the solution functions may be written in the form

$$u_r^{(0)} = \sum_{p=1}^{(1)P^{(S)}} \sum_{q=1}^4 \sum_{n=1}^2 D_{pqn}^{(1)} \overline{H}_{pq}^{(1)} f_{pq}^{(1)}(r) \sin \left\{ \zeta_p^{(1)} \theta + (n-1)\pi/2 \right\} e^{i\omega t}, \quad (34a)$$

$$u_\theta^{(0)} = \sum_{p=1}^{(1)P^{(S)}} \sum_{q=1}^4 \sum_{n=1}^2 D_{pqn}^{(1)} \overline{H}_{pq}^{(1)} g_{pq}^{(1)}(r) \cos \left\{ \zeta_p^{(1)} \theta + (n-1)\pi/2 \right\} e^{i\omega t}, \quad (34b)$$

$$u_W^{(2)} = \sum_{p=1}^{(2)P_1^{(S)}} \sum_{q=1}^2 \sum_{n=1}^2 A_{pqn}^{(2)} \overline{H}_{pq}^{(2)} \cos \left\{ \eta_{pq}^{(2)} x_2 \right\} \sin \left\{ \zeta_p^{(2)} x_1 + (n-1)\pi/2 \right\} e^{i\omega t}, \quad (35a)$$

$$u_1^{(0)} = \sum_{p=1}^{(2)P_2^{(S)}} \sum_{q=1}^2 \sum_{n=1}^2 B_{pn}^{(2)} \overline{H}_{1pq}^{(2)} \cos \left(\zeta_{pq}^{(2)} x_2 \right) \cos \left(\gamma_p^{(2)} x_1 + (n-1)\pi/2 \right) e^{i\omega t}, \quad (35b)$$

$$u_2^{(0)} = \sum_{p=1}^{(2)P_2^{(S)}} \sum_{q=1}^2 \sum_{n=1}^2 B_{pn}^{(2)} \overline{H}_{2pq}^{(2)} \sin \left(\zeta_{pq}^{(2)} x_2 \right) \sin \left(\gamma_p^{(2)} x_1 + (n-1)\pi/2 \right) e^{i\omega t}, \quad (35c)$$

$$u_1^{(0)} = \sum_{p=1}^{(3)P_1^{(S)}} \sum_{q=1}^2 \sum_{n=1}^2 B_{pqn}^{(3)} \overline{H}_{1pq}^{(3)} \sin \left(\zeta_{pq}^{(3)} x_2 \right) \cos \left(\gamma_p^{(3)} x_1 + (n-1)\pi/2 \right) e^{i\omega t} \\ + \sum_{p=1}^{(3)P_2^{(S)}} \sum_{q=1}^2 \sum_{n=1}^2 B_{pn}^{(3)} \overline{H}_{1pq}^{(3)} \cos \left(\zeta_{pq}^{(3)} x_2 \right) \cos \left(\gamma_p^{(3)} x_1 + (n-1)\pi/2 \right) e^{i\omega t}, \quad (36a)$$

$$\begin{aligned}
 u_2^{(0)} = & \sum_{p=1}^{(3)R} \sum_{q=1}^{P_1^{(S)}} \sum_{n=1}^2 B_{pqn}^{(S,A)} \overline{H}_{2pq}^{(S,A)} \cos\left(\zeta_{pq}^{(S,A)} x_2\right) \sin\left(\gamma_p^{(S,A)} x_1 + (n-1)\pi/2\right) e^{i\omega t} \\
 & + \sum_{p=1}^{(3)P_2^{(S)}} \sum_{q=1}^2 \sum_{n=1}^2 B_{pn}^{(S,S)} \overline{H}_{2pq}^{(S,S)} \sin\left(\zeta_{pq}^{(S,S)} x_2\right) \sin\left(\gamma_p^{(S,S)} x_1 + (n-1)\pi/2\right) e^{i\omega t}, \quad (36b)
 \end{aligned}$$

where $P_k^{(S)}, P_k^{(m)}, k = 1, 2, m = 2, 3$ are the numbers of dispersion curves taken, $D_{pqn}^{(S)}, A_{pqn}^{(S,S)}, B_{pn}^{(S,S)}, B_{pqn}^{(S,A)}, B_{pn}^{(S,S)}$ are unknown amplitudes to be determined (see footnote 1), $\overline{H}_{pq}^{(1)}, \overline{H}_{pq}^{(2)}$ and $\overline{H}_{kpq}^{(m)}, \overline{H}_{kpq}^{(3)}$, for $k = 1, 2, m = 2, 3$, are amplitude ratios determined from the solutions of the

homogeneous differential equations, $\zeta_p^{(1)}, \zeta_p^{(2)}, \gamma_p^{(3)}, \eta_{pq}^{(2)}, \zeta_{pq}^{(3)}$ and $\gamma_p^{(m)}, \zeta_{pq}^{(m)}$ for $m = 2, 3$, are

wavenumbers, and $f_{pq}^{(1)}(r)$ and $g_{pq}^{(1)}(r)$ are series-type vector solution functions with radial functional dependence as defined in Eqs. (31a)–(31d) of Ref. [7]. In Eqs. (34)–(36) use has been made of the fact that no flexural motion of the annular sector plate occurs in the sensing mode. All quantities appearing in Eqs. (34)–(36) are explained in detail in Sections 3 and 4 of Refs. [3,5,7]. It

should be noted that $u_1^{(0)}$ and $u_2^{(0)}$ in Eqs. (35b) and (35c) and the second terms in Eqs. (36a) and

(36b) are required in the description of the sensor because $u_r^{(0)}$ and $u_\theta^{(0)}$ in the annular sector plate

contain this motion through the power series terms $f_{pq}^{(1)}(r)$ and $g_{pq}^{(1)}(r)$. In Eqs. (34)–(36), the

symbol S in the first place of the superscript represents the sensor and A, S in the second, respectively, represent the antisymmetric and symmetric modes, if they exist. It should be noted that all the amplitudes in Eqs. (34a), (34b), (35a) and the first terms of Eqs. (36a) and (36b)⁴ must be determined from the linear algebra obtained from the variational equation that contains inhomogeneous edge and interface conditions, in accordance with footnote 1. The solution of the inhomogeneous linear algebraic equations yields the values of the unknown amplitudes and thus the solution for the vibration in the sensing direction. Since we wish to operate the tuning fork gyroscope at the fundamental natural frequency of both the actuator and the sensor, we would like both fundamental natural frequencies to be the same. In order to find these frequencies we employ Eq. (6) with Eqs. (7a), (7b) and (7c) for the actuator and Eq. (8) with Eqs. (9a), (9b) and

⁴No inhomogeneous terms occur in the variational equation associated with the second terms in (36a) and (36b).

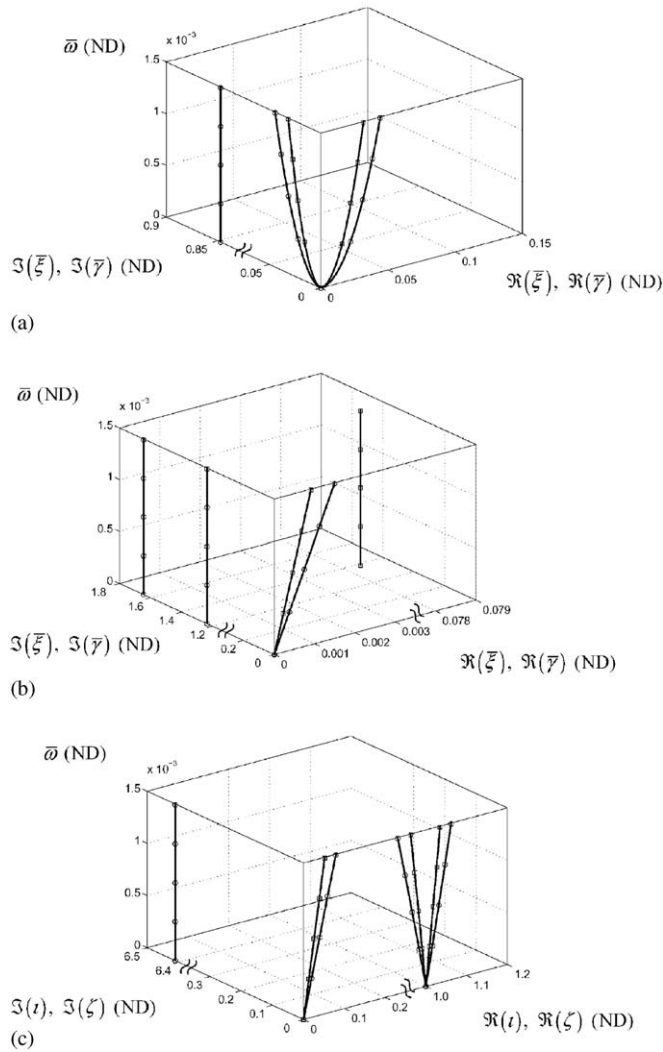


Fig. 1. Plots of dispersion curves: (a) for rectangular plate, symmetric flexure (-⊖-) and antisymmetric plane stress (-⊞-); (b) for rectangular plate, antisymmetric flexure (-⊖-) and symmetric plane stress (-⊞-); (c) for annular sector plate, flexure (-⊖-) and plane stress (-⊞-).

(9c) for the sensor, both in the homogeneous case. In this case the solutions for the actuator in Eq. (16)–(18) and for the sensor in Eqs. (34)–(36) differ in that there is an appropriate additional amplitude factor for each dispersion curve taken in each region, which we denote $F^{(S)}$. In these cases the amplitudes determined from the resulting linear algebras in the inhomogeneous cases are known from the satisfaction of the homogeneous edge conditions at the opposite free edges in each region, and the only conditions remaining in Eqs. (6) and (8) are at the interfaces and extreme edges of the configuration. The homogeneous linear algebraic equations in the $F^{(S)}$ in each case are determined from the fact that the coefficients of each $\delta F^{(S)}$ in Eq. (6) for the actuator

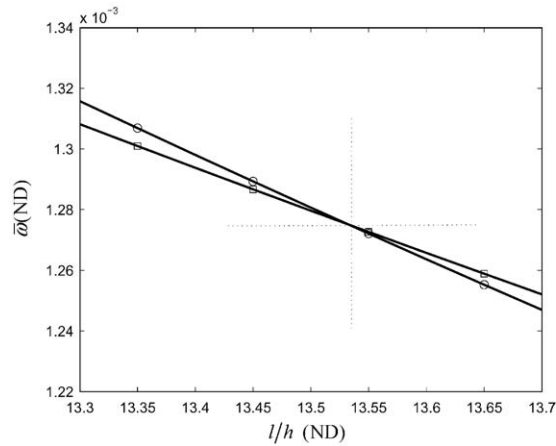


Fig. 2. Variation of the first natural frequencies of the configuration when the lengths of the rectangular plates are equal: -○-, sensing direction; -□-, actuating direction.

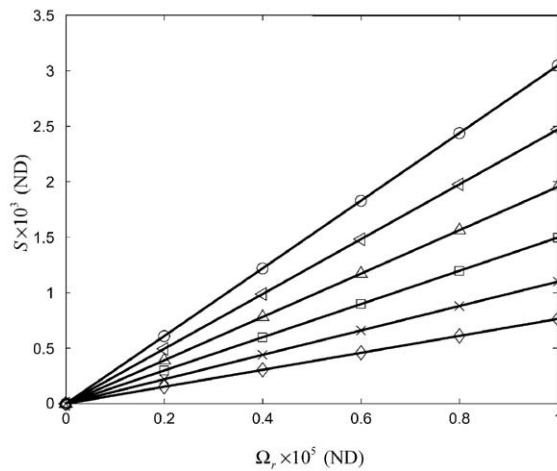


Fig. 3. Sensitivity curves of the gyroscope for different fixed Q factors (\diamond : $Q = 50$, \times : $Q = 60$, \square : $Q = 70$, \triangle : $Q = 80$, ∇ : $Q = 90$, \circ : $Q = 100$).

and in Eq. (8) for the sensor must vanish. Each linear algebra yields a transcendental determinant that must vanish. The roots of these vanishing determinants yield the eigenfrequencies for the actuating and sensing motions, respectively. We use these equations to select the geometry so that the lowest of these eigenfrequencies are the same.

3. Discussion of results

The calculation was performed using a personal computer with the symbolic mathematics package Maple [8] with quadruple precision. The piezoceramic material employed for the bimorph structures in this work is PZT-5. Detailed material properties are listed in Table VIII of

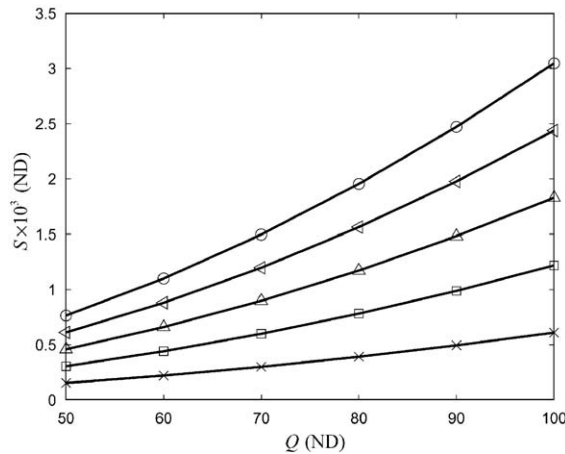


Fig. 4. Sensitivity curves of the gyroscope for different fixed rotation-rates (×: $\Omega_r = 2 \times 10^{-5}$, □: $\Omega_r = 4 \times 10^{-5}$, △: $\Omega_r = 6 \times 10^{-5}$, ◁: $\Omega_r = 8 \times 10^{-5}$, ○: $\Omega_r = 10 \times 10^{-5}$).

Ref. [9]. The thickness of each angular-rate gyroscope element is fixed at 80 μm. Also, the width to thickness ratios (b/h) of the rectangular plates and the annular sector plate are held fixed at 2.

Figs. 1(a)–(c) show the dispersion curves for the in-plane and out-of-plane motions of the rectangular and annular sector plates in the low frequency range. The abscissa in these figures represents the dimensionless frequency $\bar{\omega} = \omega/\omega_0$ (non-dimension: ND) with $\omega_0 = \pi\sqrt{c_{66}/\rho}/(2b)$ and the ordinate in Fig. 1(a) represents the dimensionless wave numbers $\bar{\gamma} = 2b\gamma/\pi$ or $\bar{\xi} = 2b\xi/\pi$ of the rectangular plate. Here, $\Re()$ and $\Im()$ represent real and imaginary parts of the arguments, respectively. Based on the range of interest of the first natural frequency, we take two dispersion branches for vibration in plane stress and three branches for the flexural vibration of the rectangular plate for both symmetric and antisymmetric modes, and three dispersion branches for the vibration in plane stress and four branches for the flexural vibration of the annular sector plate.

The same fundamental natural frequencies for both sensor and actuator motion directions enable not only the reduction of the driving force but also cause the largest vibration in the sensing direction for a given vibration in the actuating direction. In order to find the geometry for the fundamental natural frequency to be the same, some tentative calculations were conducted first to narrow the range of the geometry considered.

The configuration treated in this work has much merit, as a result of the smooth change in direction of the tangent vector in the plane of the annular sector plate, as opposed to an abrupt change. Furthermore, the symmetric structure of the configuration keeps the vibratory motion in the sensing direction self-balanced; hence, the vibratory energy in the tines would not be readily transmitted and dissipated through the support structure.

The length of the tine, composed of the two rectangular plates of equal length, is varied to find a matched fundamental natural frequency of the system for both actuating and sensing. Fig. 2 exhibits a crossover point of the fundamental natural frequencies in both directions, which means that the fundamental natural frequencies of the system in both actuating and sensing directions are equal. Note that the lengths of both rectangular plates are kept equal. The abscissa in the figure represents the lengths of the plates. This figure shows that the lengths of the plates with a

matched frequency⁵ $\bar{\omega} \approx 1.275 \times 10^{-3}$ are $l/h \approx 13.53$ ($\omega/2\pi \approx 6.8$ kHz, $l \approx 0.54$ mm). Furthermore, the ratio of the radius to the half thickness of the annular sector plate, which is the measure of the length from the center of the annular sector to the mid-line of the plate, is $r_0/h = 9$. Here the connecting pieces with the same density as the plates were employed between volume (1) and (2) as well as between volume (2) and (3). The thickness ratio of each connecting element to the thickness of the plate (t_c/h) is fixed at 1. Since $|\Omega| \ll \omega$, the decoupling procedure employed is very accurate. Fig. 3 shows the calculated sensitivity of the gyroscope with rotation-rate for values of Q ranging from 50 to 100. The sensitivity S has been defined as the ratio of the current induced in the sensing plate to the current in the actuating plate, i.e., $S = |I_S^{(m)}|/|I_A^{(m)}|$, $m = 1, 2$. In Fig. 3,

Ω_r has been defined as the rotation-rate Ω normalized by the actuating frequency ω or $\Omega_r = \Omega/\omega$ (ND). The response of the vibratory gyroscopes near resonance depends on the quality factor Q of the vibrator. Since Q cannot be calculated, it must be measured. Consequently, the calculations have been performed for the range of values of Q shown in the figure. As expected the sensitivity increases with increasing Q .

Fig. 4 shows the calculated sensitivity of the vibratory gyroscope with Q for values of Ω_r ranging from 2×10^{-5} to 10×10^{-5} , which corresponds to rotation-rates Ω ranging from 8 to 41 RPM, and is not to be regarded as a limitation. As can be seen in this figure, the sensitivities increase with increasing Q factor.

References

- [1] Jongwon Seok, H.F. Tiersten, H.A. Scarton, An analysis of a vibratory angular-rate gyroscope using polarized piezoceramic bimorph plates. Part 1: derivation of variational equations in the absence of angular velocity, *Journal of Sound and Vibration* 280 (1–2) (2005) 263–287.
- [2] C. Lanczos, *The Variational Principles of Mechanics*, University of Toronto Press, Toronto, 1949 (Chapter IV).
- [3] Jongwon Seok, H.F. Tiersten, H.A. Scarton, Free vibrations of rectangular cantilever plates. Part 1: out-of-plane motion, *Journal of Sound and Vibration* 271 (1–2) (2004) 131–146.
- [4] Jongwon Seok, H.F. Tiersten, Free vibrations of annular sector cantilever plates. Part 1: out-of-plane motion, *Journal of Sound and Vibration* 271 (3–5) (2004) 757–772.
- [5] Jongwon Seok, H.F. Tiersten, H.A. Scarton, Free vibrations of rectangular cantilever plates. Part 2: in-plane motion, *Journal of Sound and Vibration* 271 (1–2) (2004) 147–158.
- [6] H.F. Tiersten, *Linear Piezoelectric Plate Vibrations*, Plenum Press, New York, 1969 Section 8.5.
- [7] Jongwon Seok, H.F. Tiersten, Free vibrations of annular sector cantilever plates. Part 2: in-plane motion, *Journal of Sound and Vibration* 271 (3–5) (2004) 773–787.
- [8] Maple™ V, *User Manual Release 5*, Waterloo Maple Inc., Ontario, Canada, 1997.
- [9] W.P. Mason, *Physical Acoustics*, Vol. 1, Part A, Academic Press, New York, 1964, pp. 202–204.

⁵The angular velocity Ω has been ignored when the geometry is selected so that the fundamental natural frequencies of the actuating motion and sensing motion are made the same because Ω is a variable and it is not meaningful to include it. When the variable Ω , which is to be measured by the device, is included it separates the equal frequencies a small amount. If the Q is not sufficiently small, the broadened response will exhibit two small peaks caused by the separation in natural frequencies. However, if the Q is sufficiently small, the broadened response will show only one peak. Although the gyroscope measures current and not frequency, this consideration has significant implication in the use of the device.